sustainability

MDPI

Article

Future Projection of Precipitation Bioclimatic Indicators over Southeast Asia Using CMIP6

Mohamed Tarek Sobh [1], Mohammed Magdy Hamed [1,2], Mohamed Salem Nashwan [3,*] and Shamsuddin Shahid [2]

[1] Construction and Building Engineering Department, College of Engineering and Technology, Arab Academy for Science, Technology and Maritime Transport (AASTMT), B 2401 Smart Village, 12577 Giza, Egypt
[2] Department of Water and Environmental Engineering, School of Civil Engineering, Faculty of Engineering, Universiti Teknologi Malaysia (UTM), Skudia 81310, Malaysia
[3] Construction and Building Engineering Department, College of Engineering and Technology, Arab Academy for Science, Technology and Maritime Transport (AASTMT), 2033 Elhorria, Cairo 11736, Egypt
* Correspondence: m.salem@aast.edu

Abstract: Precipitation is a key meteorological component that is directly related to climate change. Quantifying the changes in the precipitation bioclimate is crucial in planning climate-change adaptation and mitigation measures. Southeast Asia (SEA), home to the world's greatest concentration of ecological variety, needs reliable monitoring of such changes. This study utilized the global-climate models from phase 6 of coupled model intercomparison project (CMIP6) to examine the variations in eight precipitation bioclimatic variables over SEA for two shared socioeconomic pathways (SSPs). All indicators were studied for the near (2020–2059) and far (2060–2099) futures to provide a better understanding of the temporal changes and their related uncertainty compared to a historical period (1975–2014). The results showed a high geographical variability of the changes in precipitation-bioclimatic indicators in SEA. The mainland of SEA would experience more changes in the bioclimate than the maritime region. The multimodel ensemble (MME) showed an increase in mean annual rainfall of 6.0–12.4% in most of SEA except the Philippines and southern SEA. The increase will be relatively less in the wettest month (15%) and more in the driest month (20.7%) in most of SEA; however, the precipitation in the wettest quarter would increase by 2.85%, while the driest quarter would decrease by 1.0%. The precipitation would be more seasonal. In addition, the precipitation would increase over a larger area in the wettest month than in the driest month, making precipitation vary more geographically.

Keywords: precipitation extremes; shared socioeconomic pathways; GCM; SEA; climate change

Citation: Sobh, M.T.; Hamed, M.M.; Nashwan, M.S.; Shahid, S. Future Projection of Precipitation Bioclimatic Indicators over Southeast Asia Using CMIP6. *Sustainability* **2022**, *14*, 13596. https://doi.org/10.3390/su142013596

Academic Editor: Baojie He

Received: 30 September 2022
Accepted: 19 October 2022
Published: 20 October 2022

1. Introduction

Precipitation is the most crucial climatic factor for the ecosystem. It is the primary factor of floods, droughts, erosions, and other hydrological water-related disasters. It also defines the ecological conditions that allow for the proliferation of various species over a given area. Precipitation-bioclimatic indicators explain the interplay between environmental wetness/dryness and living things [1]. The precipitation bioclimate influences biodiversity, vegetation cover, ecology, and irrigation requirements. It is crucial for sustainability because it characterizes the agricultural potential, species distribution, public heat risk, and pollution susceptibility [2–4]. Variations in rainfall and consequent changes in temperature and humidity impact the human ability to maintain an energy balance and comfort [5]. It has also been used to quantify a region's potential for cultivating a desired crop [6]. Most species require a certain range and variability of rainfall to survive; therefore, rainfall is the major driver of an area's species distribution and ecology [7,8]. Precipitation is also highly linked with disease outbreaks and fatality rates [9,10]. Air pollution and environmental conditions are also dependent on precipitation [11].

Global-warming-induced climate change has altered the precipitation regime around the world by amplifying the hydrological cycle [12]. The alteration in mean precipitation has also caused a variation in seasonal, temporal and spatial precipitation patterns, adversely impacting agricultural products, the environment, water sustainability, the national economy, and people's livelihoods. Even a little change in the bioclimate can significantly affect the bio-environment and biological distribution [13]. As precipitation provides an understanding of a region's bio-environment, trends in precipitation-related-bioclimatic indicators can foretell the anticipated alterations of its biodiversity; therefore, precipitation-related-bioclimatic indicators must be analyzed to understand the possible biological reactions of climate change so we can propose the required adaptation or mitigation actions [13].

The shifts in the precipitation bioclimate vary greatly between locations; therefore, it is crucial to evaluate how the precipitation bioclimate has changed in regions with a wide range of climatic and topographical conditions. Southeast Asia (SEA) has a diverse geography with numerous highlands, plains and islands. It has one of the world's greatest densities of tropical species [14,15]. The considerable biodiversity has narrowed the niches of tropical species. The region has experienced a climatic shift over the past few decades [16,17]. This has caused a significant disturbance of species niches in the region; therefore, some of SEA's regions have been classified as the home of irreplaceable and threatened species due to climate change [18–20]. Numerous micro-interactions between the ocean, land, and atmosphere make SEA's climate highly complex [21]. The topographical and climate variabilities have made the hydrological systems extremely sensitive. This has made it one of the world's most climate-vulnerable regions. Four countries in SEA ranked among the world's ten most vulnerable to climate change during 1997–2016 [21,22]. Recent increases in flood danger have provided a significant obstacle to development, especially in Malaysia; therefore, it is essential to understand the effects of climate change on the region.

Several studies have evaluated the changing climate in SEA based on different climate variables, such as mean temperature, rainfall, extreme rainfall/temperature, and seasonal rainfall/temperature;however, these variables are insufficient to identify the specific factors determining biological and ecological changes. Correlational niche analysis techniques, widely used for species-occurrence modeling, depend on statistical relationships between species occurrences and environmental factors [23]. Different bioclimatic variables have been identified as driving environmental factors of species occurrences. For this purpose, the bioclimatic variables are available from WorldClim [24] and ENVIRIM [25]. The WorldClim bioclimatic variables can best explain the climate influence on a species' physiology and ecology [24,26]; therefore, they are most widely employed for assessing the present- and future-precipitation bioclimatology [26–28]. There are no particular studies available right now that project precipitation-bioclimatic variables in tropical SEA.

Climate change impacts are generally evaluated using global climate model (GCMs) simulations [29]. These GCMs are developed under the coupled model intercomparison projects (CMIPs) [30]. Due to GCMs being generated by various organizations/research groups, their performance varies globally, and various degrees of uncertainty are associated with each of them. The latest version of CMIP, CMIP6, gives a more realistic depiction of Earth's physical processes than earlier CMIPs [31]. GCMs relied on robust projection scenarios known as shared socioeconomic pathways (SSPs), the updated version of representative concentration pathways (RCPs) [32]. There is less uncertainty in CMIP6 GCMs' future projection than in the previous version [33]. Several studies showed better performance of the CMIP6 model for SEA. Iqbal et al. [34] ranked the performance of 35 GCMs from CMIP6 using compromised programming from 1975 to 2014 in the mainland of SEA. The results illustrated that most CMIP6 GCMs could capture and simulate the precipitation climatological data. Hamed et al. [35] compared 13 GCMs from CMIP6 with their predecessor from CMIP5 in simulating historical precipitation projections over SEA. They concluded that the CMIP6 simulations have less uncertainty than CMIP5.

This study employed eight bioclimatic precipitation indicators of WorldClim to quantify the future bioclimatic changes in SEA for the intermediate (SSP2-4.5) and pessimistic (SSP5-8.5) scenarios using 23 CMIP6 GCMs. The findings of this study will help scientists better understand how precipitation indices are significant to the bio-environment, agriculture, water resources, and wildlife distribution of SEA. Additionally, the results may help policymakers in SEA establish suitable climate-change mitigation and adaptation methods.

2. Data and Sources

2.1. Study Area

SEA is located between latitude −10°–30° N and longitude 90°–141° E and encompasses an area of 4,550,000 km^2, including 11 countries. Figure 1 depicts its topography, measured in meters, above the mean sea level. Some areas in Myanmar and Indonesia have elevations up to 4000 m above sea level, but the rest of the region is mainly flat. The mean annual precipitation ranges between 750 to 5000 mm [35]. Its climate is equatorial, with a constant temperature, high humidity, and heavy precipitation. Solar radiation has a low incidence angle, meaning temperatures do not significantly fluctuate throughout the year [21]. Climate extremes, such as droughts and floods, are widespread in most SEA because of the complex spatiotemporal atmospheric dynamics.

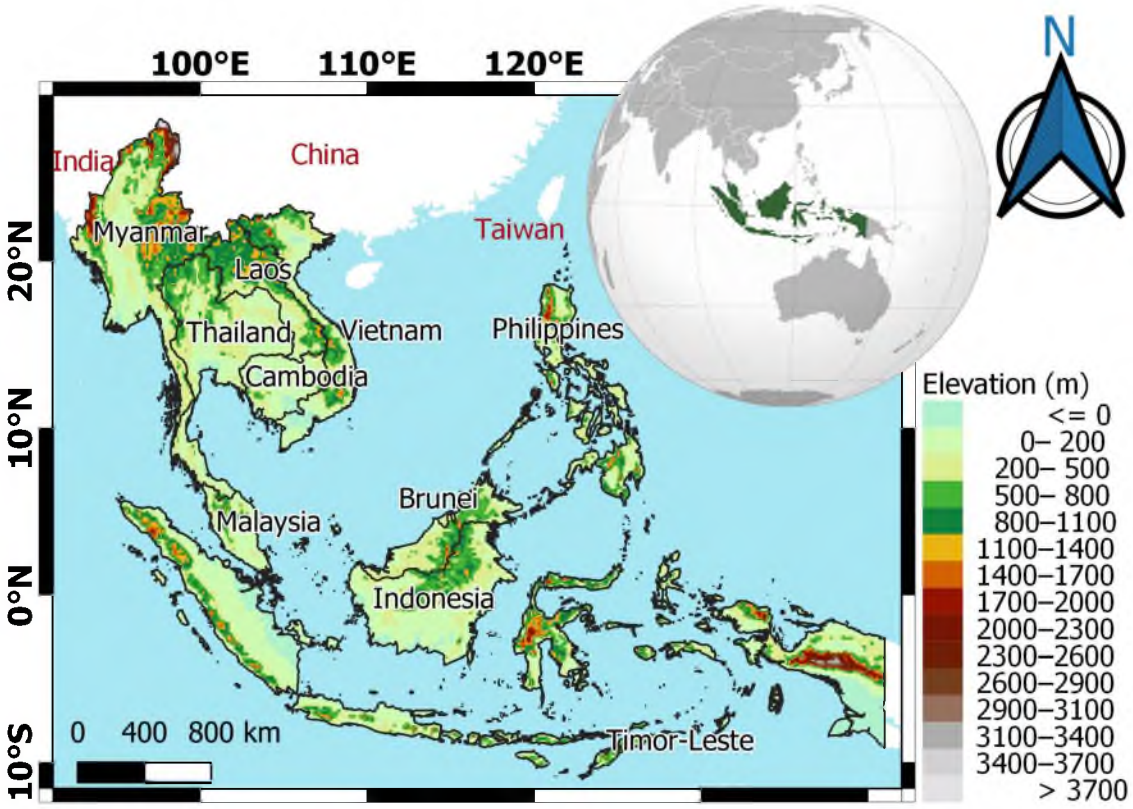

Figure 1. The location and topography of Southeast Asia.

2.2. Global Climate Models (GCMs)

The CMIP6 GCMs model's extracted outputs yielded historical and future climate simulations from 1975 to 2099 (https://esgf-node.llnl.gov/search/cmip6/ (accessed on 20 March 2022)). Table 1 shows the 23 models that were used. All the models consider one initialization variant label as r1i1f1p1. The simulations from two scenarios were selected, i.e., SSP2-4.5 and SSP5-8.5. The SSP2-4.5 scenario represents the emissions of greenhouse gases to be kept at a moderate level. The SSP5-8.5 scenario represents the use of a rapidly evolving planet powered by fossil fuels emitting large amounts of greenhouse gases [36].

Accordingly, the two projections can reflect the wide range of climate characteristics resulting from two pathways under global warming.

Table 1. CMIP6 GCMs used in the study.

No.	Model	Institution	Country	Original Spatial Resolution
1	ACCESS-CM2	CSIRO-ARCCSS	Australia	1.87 × 1.25°
2	ACCESS-ESM1-5			1.875 × 1.25°
3	AWI-CM-1-1-MR	AWI	Germany	0.93 × 0.93°
4	BCC-CSM2-MR	BCC	China	1.12 × 1.12°
5	CanESM5	CCCMA	Canada	2.79 × 2.81°
6	CAS-ESM2-0	CAS-ESM	China	1.40 × 1.40°
7	CIESM	CIESM	China	0.90 × 1.30°
8	CMCC-ESM2	CMCC	Italy	0.94 × 1.25°
9	EC-Earth3	EC-Earth	Europe	0.35 × 0.35°
10	EC-Earth3-CC			0.35 × 0.35°
11	EC-Earth3-Veg			0.35 × 0.35°
12	EC-Earth3-Veg-LR			0.35 × 0.35°
13	FGOALS-g3	FGOALS	China	2.00 × 2.00°
14	FIO-ESM-2-0	FIO	China	1.25 × 0.90°
15	GFDL-ESM4	NOAA-GFDL	USA	1.00 × 1.25°
16	INM-CM4-8	INM	Russia	2.00 × 1.50°
17	INM-CM5-0			2.00 × 1.50°
18	IPSL-CM6A-LR	IPSL	France	2.50 × 1.27°
19	MIROC6	MIROC	Japan	1.40 × 1.40°
20	MPI-ESM1-2-HR	MPI-M	Germany	0.94 × 0.94°
21	MPI-ESM1-2-LR			1.87 × 1.86°
22	MRI-ESM2-0	MRI	Japan	1.12 × 1.12°
23	NESM3	Nanjing University	China	1.90 × 1.90°

3. Methodology

This study attempted to examine the future changes in SEA's precipitation bioclimate. Table 2 provides detailed explanations for the bioclimatic indicator used. The MME mean represents the 90% confidence interval (CI) or 5th, and 9th percentiles for each indicator were estimated using 23 GCMs. The outputs of the GCMs were interpolated to 1.0° spatial resolution using bilinear interpolation, as used in many studies [37]. It was employed to calculate the bioclimatic indicators for the historical (1975–2014) as well as for two future periods, near (2020–2059) and far (2060–2099). The expected changes in bioclimatic indicators for various periods were estimated at each grid point. The results were computed for two projected scenarios, SSP2-4.5 and SSP5-8.5. The dynamic method was used for Bio-13 to Bio-19, except Bio-15, to select the month and three consecutive months with the maximum and minimum temperature/precipitation for both historical and future periods. The selection of the driest/wettest month/quarter was not fixed, meaning reselection occurred for a future period [38].

Table 2. Detailed explanations of the precipitation bioclimatic indicators used in this study.

Indicator	Equation	Unit
Bio-12 Annual precipitation	$\text{Bio}-12=\sum_{i=1}^{i=12} PPT_i$	mm
Bio-13 Precipitation in the wettest month	$\text{Bio}-13=\max([PPT_i,\ldots,PPT_{12}])$	mm
Bio-14 Precipitation in the driest month	$\text{Bio}-14=\min([PPT_i,\ldots,PPT_{12}])$	mm
Bio-15 Precipitation seasonality	$\text{Bio}-15=\frac{SD\ \{PPT_i,\ldots,PPT_{12}\}}{1+\left(\frac{\text{Bio }12}{12}\right)}\times 100$	%
Bio-16 Precipitation in the wettest quarter	$\text{Bio}-16=\max\left(\left\vert\begin{array}{c}\sum_{i=1}^{i=3} PPT_i,\\ \sum_{i=2}^{i=4} PPT_i,\\ \ldots,\\ \sum_{i=10}^{i=12} PPT_i,\\ \sum_{i=11}^{i=1} PPT_i,\\ \sum_{i=12}^{i=2} PPT_i,\end{array}\right\vert\right)$	mm
Bio-17 Precipitation in the driest quarter	$\text{Bio}-17=\min\left(\left\vert\begin{array}{c}\sum_{i=1}^{i=3} PPT_i,\\ \sum_{i=2}^{i=4} PPT_i,\\ \ldots,\\ \sum_{i=10}^{i=12} PPT_i,\\ \sum_{i=11}^{i=1} PPT_i,\\ \sum_{i=12}^{i=2} PPT_i,\end{array}\right\vert\right)$	mm
Bio-18 Precipitation in the warmest quarter	$Q_{Tmax}=\max\left(\left\vert\begin{array}{c}\sum_{i=1}^{i=3} Tavg_i,\\ \sum_{i=2}^{i=4} Tavg_i,\\ \ldots,\\ \sum_{i=10}^{i=12} Tavg_i,\\ \sum_{i=11}^{i=1} Tavg_i,\\ \sum_{i=12}^{i=2} Tavg_i,\end{array}\right\vert\right)$	mm
	$\text{Bio}-18=$ $\sum_{i=1}^{i=3} PPT_i$, based on the three selected months of Q_{Tmax}	

Table 2. *Cont.*

Indicator	Equation	Unit
Bio-19 Precipitation in the coldest quarter	$Q_{Tmin} = \min\left(\left\{\sum_{i=1}^{i=3} Tavg_I, \sum_{i=2}^{i=4} Tavg_I, \ldots, \sum_{i=10}^{i=12} Tavg_I, \sum_{i=11}^{i=1} Tavg_I, \sum_{i=12}^{i=2} Tavg_I\right\}\right)$ $\text{Bio} - 19 =$ $\sum_{i=1}^{i=3} PPT_i$, based on the three selected months of Q_{Tmin}	mm

PPT is defined as the total precipitation of a single month. i is the number of the month in the year. T_{max} is the monthly mean of daily maximum temperatures in °C. T_{min} is the monthly mean of daily minimum temperatures in °C.

4. Results

MME was formed using the historical and future projections of precipitation bioclimatic indicators (Table 2) using the available GCMs. These sections detail the historical MME mean values for each indicator. Aside from that, this section presents the 5th, 95th, and mean values of the projected changes of the indicators for SSP2-4.5 and SSP5-8.5. The 90% CI is shown by comparing the 5th and 95th percentiles. In addition, eight rainfall bioclimatic indicators were computed for ACCESS-CM2, as an example, for comparison, as presented in the Supplementary Materials.

4.1. Mean Annual Precipitation

The spatial distribution of the mean annual precipitation (Bio-12) for historical and future periods is illustrated in Figure 2. The historical mean annual precipitation ranged from 1500 to 4000 mm, except for middle Myanmar and the southeastern region, where it was the lowest and highest, respectively. In Myanmar, precipitation ranged from 1200 to 2000 mm, and 4000 to 5500 mm in the southeast region. The projected MME mean of Bio-12 for SSP2-4.5 and SSP5-8.5 were nearly identical in the near and far futures. The projected mean from Bio-12 revealed an increase of 6–12.4% in most SEA, except the southern part and the Philippines. Rainfall was projected to decrease by 5.5 and 6.4% in those regions for near and far futures, respectively, for SSP2-4.5. It was nearly identical to SSP5-8.5. In the near and far futures, the projections of the 5th and 95th percentiles were identical between SSP2-4.5 and SSP5-8.5. The 5th percentile showed decreased annual precipitation by −15 to −65% over all of SEA. The greatest decrease was in northern Myanmar, and the lowest decrease was in Laos and eastern Thailand. The 95th percentile map illustrated an increase of 20 to 200%. The largest increase was in northern Myanmar. The areal averages of the 5th and 95th percentiles for different scenarios were similar for the near and far futures.

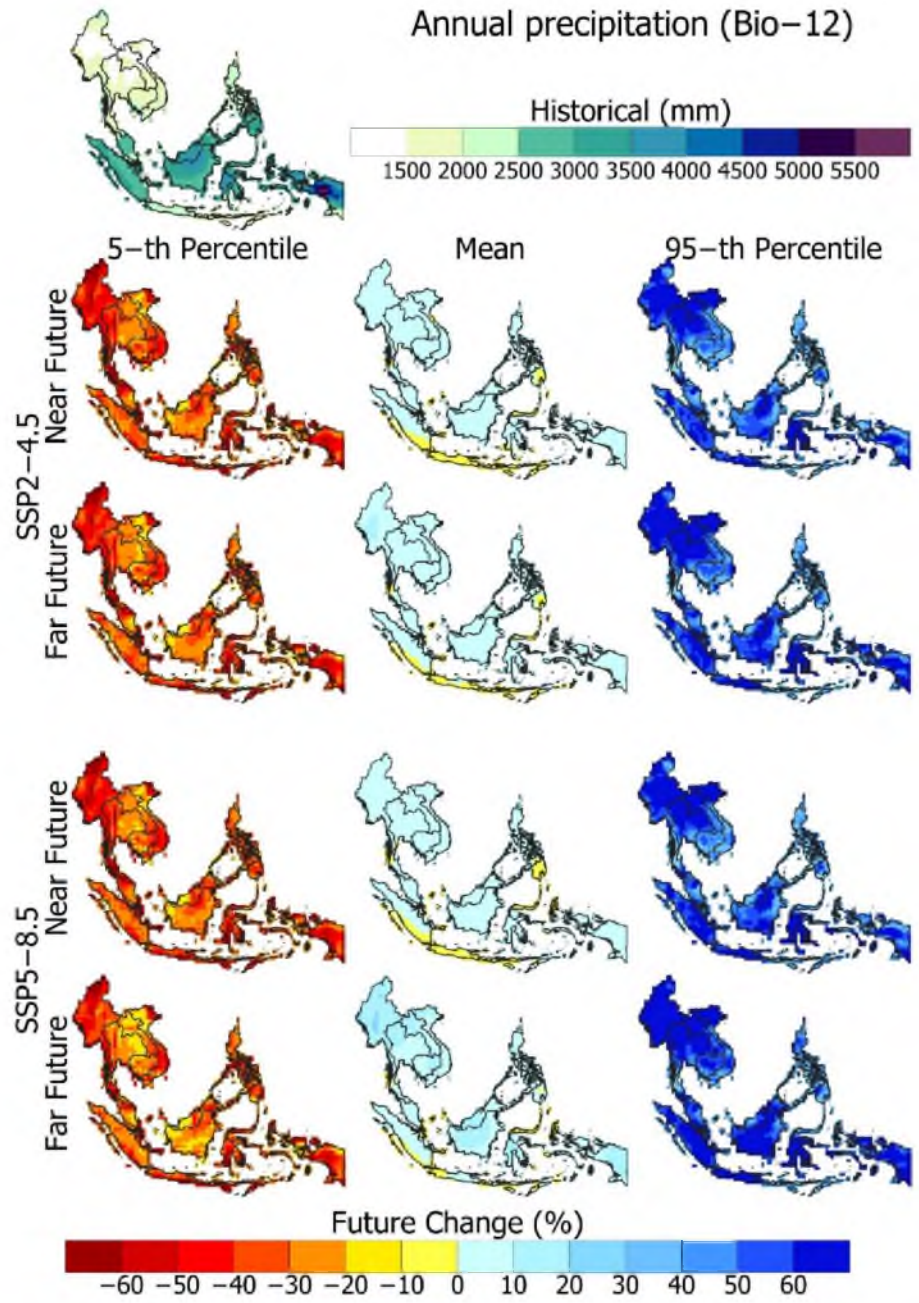

Figure 2. Spatial distribution of historical mean annual precipitation (Bio-12) and its changes in the near and far futures for SSP2-4.5 and SSP5-8.5.

4.2. Precipitation of Wettest Month (Bio-13)

The spatial distribution of the historical and future precipitation in the wettest month was prepared by identifying the month with the maximum cumulative precipitation at each grid point (Figure 3). The historical precipitation in SEA ranged from 320 to 500 mm in most of SEA, except in southern Myanmar and southeastern SEA where it ranged from 500 to 650 mm. The MME mean of the projected Bio-13 revealed a small increase in most SEA by 15% except for southern regions and western Indonesia in the near future of SSP2-4.5. In addition, an increase was projected in SEA in the far future, except for the southern coastal regions. For SSP5-8.5, Bio-13 showed an increase over the whole of SEA for both futures, except in southern coastal areas, northwestern Indonesia, and eastern SEA for the near future. The far future presented the highest increase in Myanmar by 30.6%. The 5th percentile maps revealed a decrease of up to 65% over all of SEA. The changes

in both futures for SSP2-4.5 and the near future for SSP5-8.5 were nearly identical. The projected MME mean for SSP5-8.5 (far future) showed the lowest decrease in Thailand, Laos, and Indonesia. The MME for 95th revealed an increase of up to 165% over all of SEA. The highest increase would be in Myanmar for both futures and scenarios.

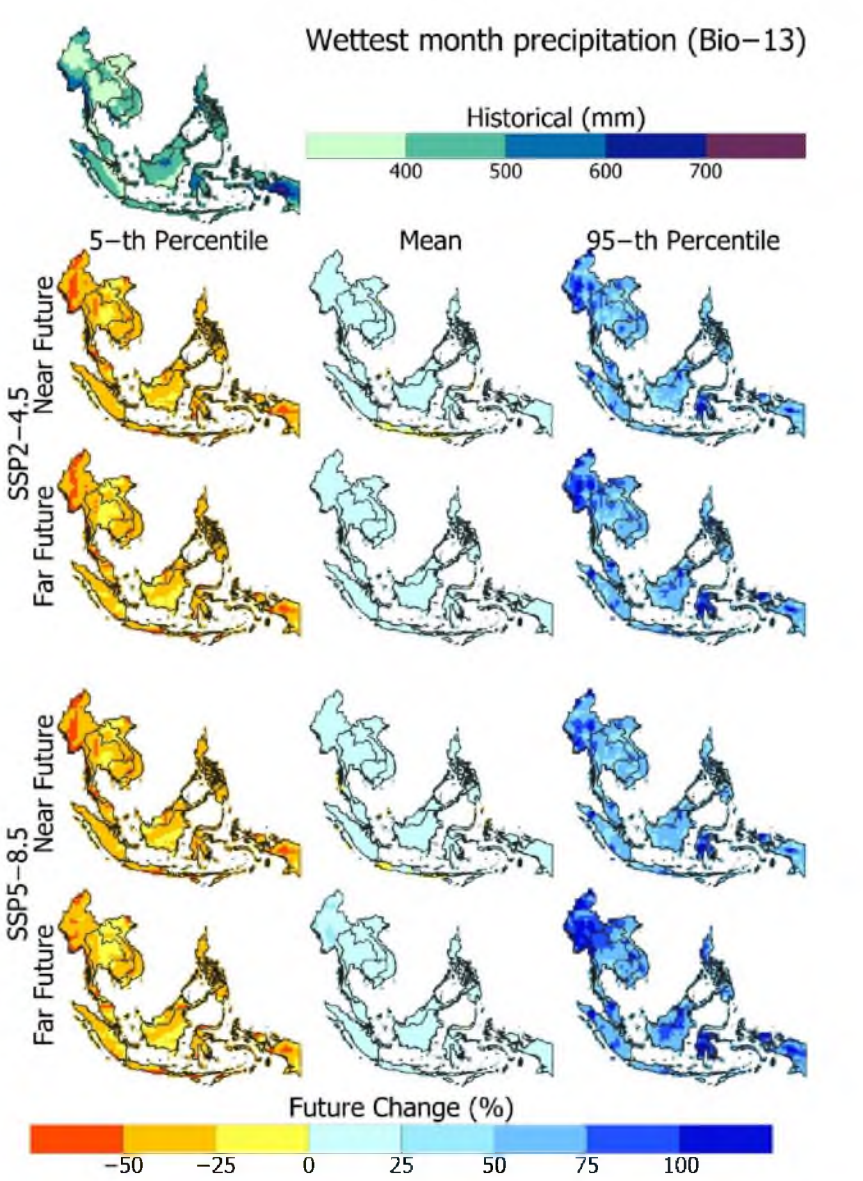

Figure 3. Spatial distribution of historical mean precipitation of the wettest month (Bio-13) and its changes in the near and far futures for SSP2-4.5 and SSP5-8.5.

4.3. Precipitation of Driest Month (Bio-14)

Bio-14 was calculated by finding the month with the lowest cumulative precipitation amount. The spatial patterns of historical and future changes in Bio-14 are illustrated in Figure 4. During the historical period, Bio-14 showed the lowest precipitation over northwestern SEA by 0 to 25 mm, and the highest observed in the Southeast by 150 to 200 mm. The MME mean projected Bio-14 was nearly identical for the near and far future under both scenarios. For SSP2-4.5, the MME showed changes of 19 to 23% for the near future and −26 to 30% for the far future. For SSP5-8.5, the MME showed changes of −21.1 to 18.4% and −36.4 to 20.7% for the near and far futures, respectively. The 5th percentile maps showed an overall decrease in SEA for the two scenarios. The lowest decrease was observed in central Indonesia, southwestern SEA, and the southeastern

coastal region of SEA. The 95th percentile projection illustrated a similarity between the two scenarios in both futures. The MME revealed an increase of 25.1 to 696.8% for near futures and 26.1 to 919.3% for far futures under both scenarios. The highest increase was observed in the southern Myanmar and Thailand.

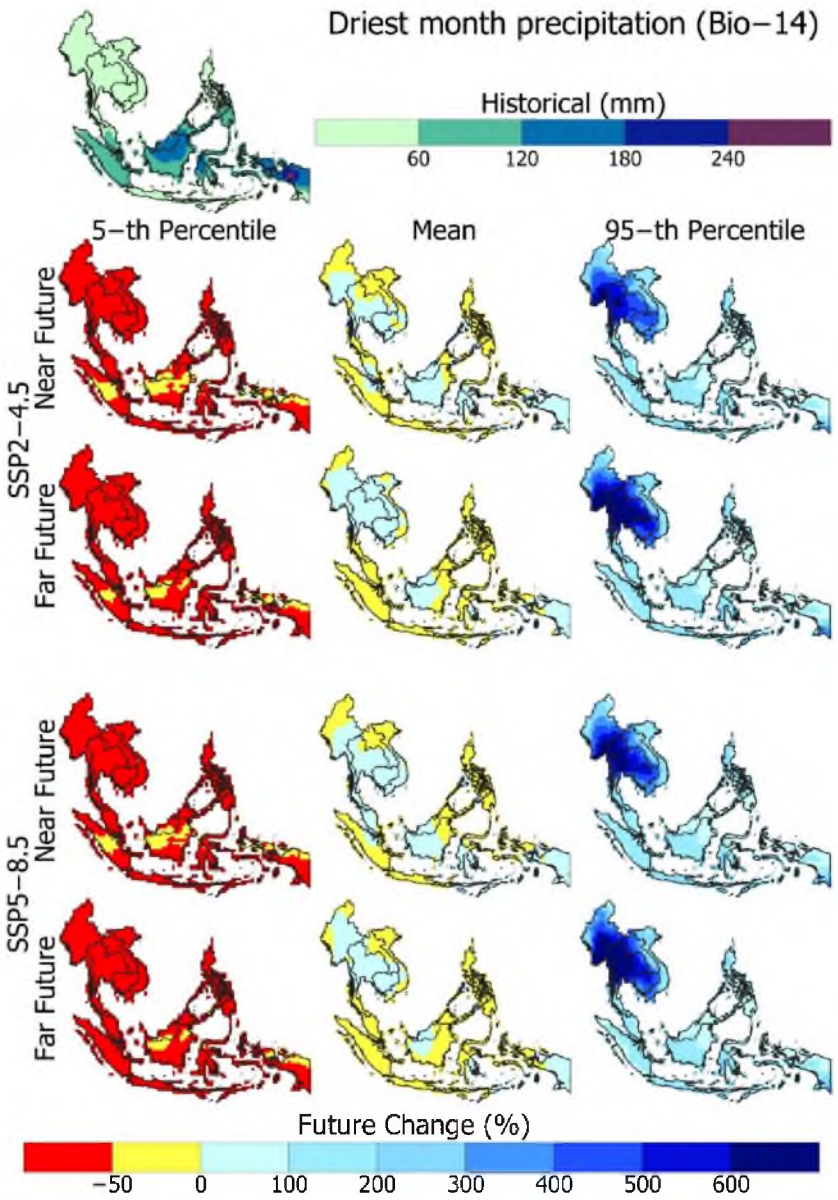

Figure 4. Spatial distribution of historical mean precipitation driest month (Bio-14) and its changes in the near and far futures for SSP2-4.5 and SSP5-8.5.

4.4. Precipitation Seasonality (Bio-15)

The variation in monthly precipitation totals over a year is represented using Bio-15. The spatial distributions of Bio-15 for the reference and future periods are illustrated in Figure 5. Bio-15 ranged from 25 to 125% for the historical period. The highest value was in Myanmar and the southern region of SEA. For SSP2-4.5, an increase in mean Bio-15 was projected, ranging from 0.0 to 6.0% and −0.7 to 8.4% for the near and far future, respectively; however, a decrease was observed in Brunei by −1.3% in the near future. For SSP5-8.5, MME mean projection of Bio-15 for the near future showed an identical distribution pattern to SSP2-4.5's far future. The highest increase would be in the far future in the southwestern coastal region. The 5th percentile illustrated a decrease over SEA ranging from −5.0 to

−50.0% for all scenarios, with the highest decrease in the south of Myanmar, Thailand, Cambodia, and Vietnam. The lowest decrease was in the northern Brunei and Indonesia. The 95th showed an increase ranging from 10 to 65%, with the highest increase in the northern and southern coastal regions.

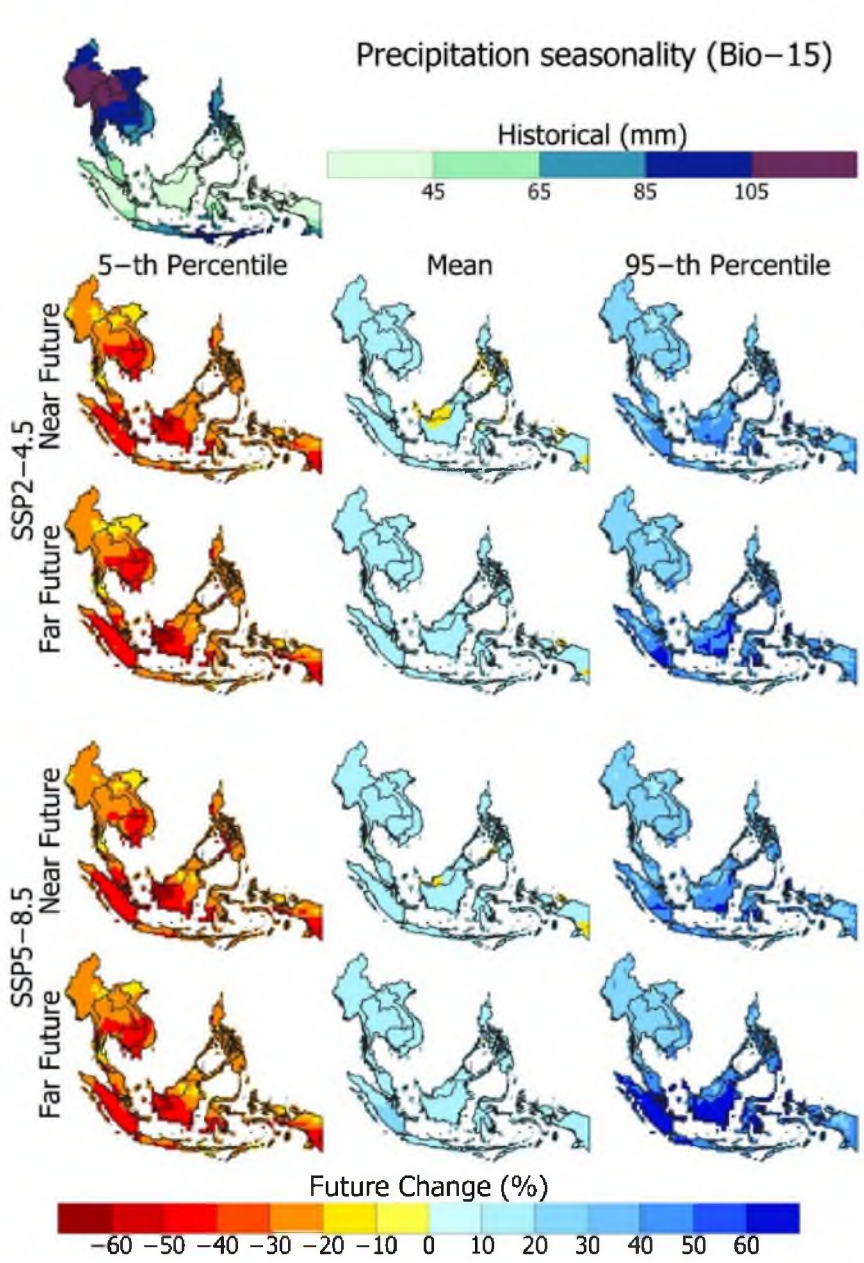

Figure 5. Spatial distribution of historical mean precipitation seasonality (Bio-15) and its changes in the near and far futures for SSP2-4.5 and SSP5-8.5.

4.5. Precipitation of Wettest and Driest Quarter

Interpretations of total precipitation during the wettest and driest consecutive three months of the year are provided by Bio-16 and Bio-17. These two indicators can be used to examine how such environmental conditions may alter the seasonal distributions of species. Total precipitation for the wettest and driest consecutive three months is illustrated in Figures 6 and 7, respectively. During the historical period, Bio-16 values ranged from 744 to 1600 mm, where the highest values were in southern Myanmar and southeastern SEA. The Bio-17 ranged from 75 to 720 mm, with the highest in Brunei, Indonesia, and southeastern SEA.

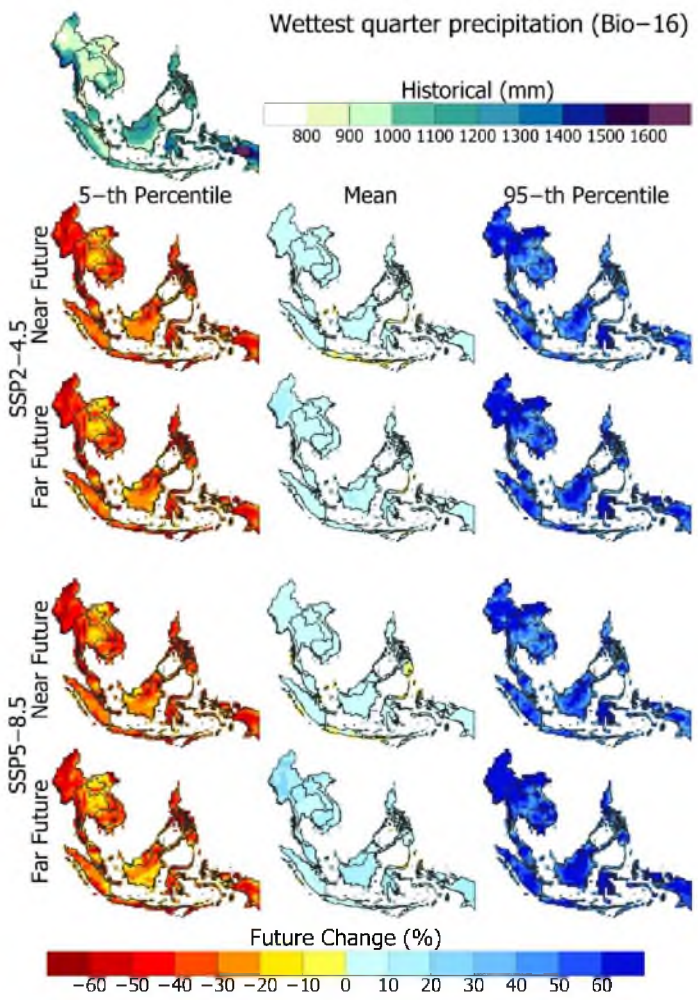

Figure 6. Spatial distribution of historical mean precipitation of wettest quarter (Bio-16) and its changes in the near and far futures for SSP2-4.5 and SSP5-8.5.

The projected MME mean (CI) of Bio-16 showed an increase of 2.85% (−36.1 to 52.3%) in the near future and 5.9% (−35.20 to 57.70%) in the far future for SSP2-4.5. For the SSP5-8.5 scenario, Bio-16 was projected to increase by 3.06% (−36.06 to 53.11%) in the near future and 9.04% (−33.7 to 63.1%) in the far future. For Bio-17, MME mean projection showed a decrease over the entire SEA by 1.04% (−69.24 to 143.89%) in the near future and 0.83% (−70.85 to 158.17) in the far future for SSP2-4.5. For SSP5-8.5, Bio-17 showed an increase of 0.17% (−69.9 to 158.17%) in the near future and a decrease of 2.30% (−73.66 to 157.45%) in the far future. Bio-17 showed a decrease in most of SEA, except in Indonesia, central SEA mainland, and the southeastern islands, where Bio-17 was projected to increase for both scenarios. The 5th and 95th percentile for Bio-16 showed the highest increase and decrease in northern Myanmar. The highest uncertainty and fluctuations were in northern Myanmar between the 5th and 95th percentile for these two indicators.

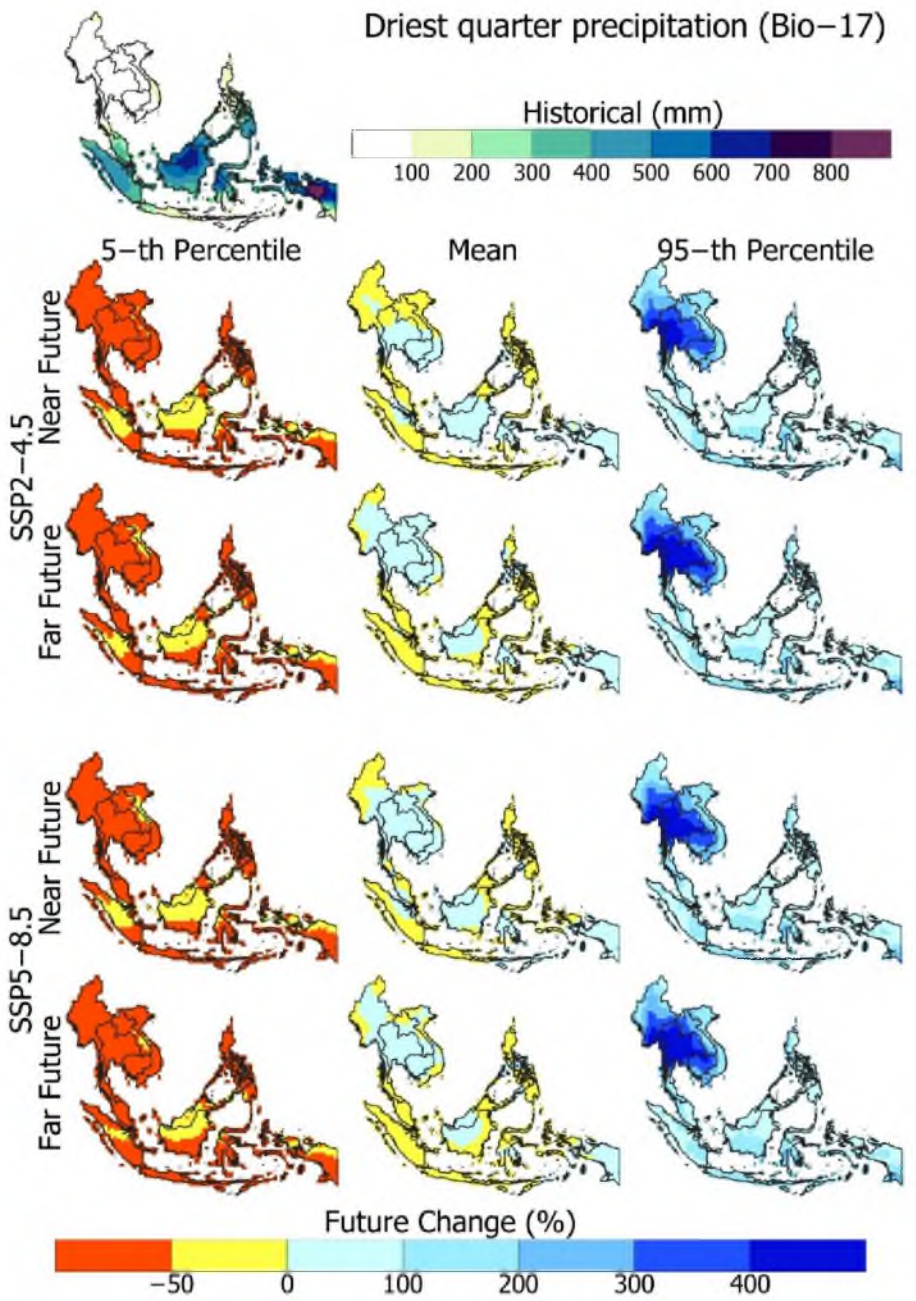

Figure 7. Spatial distribution of historical mean precipitation of driest quarter (Bio-17) and its changes in the near and far futures for SSP2-4.5 and SSP5-8.5.

4.6. Precipitation of Warmest and Coldest Quarter

Bio-18 and Bio-19 were calculated by determining the warmest and coldest quarters. The average temperature of each three consecutive month groupings was summed to select the highest and lowest quarter values, and then the total precipitation of the selected quarter was calculated. The indicators for the historical and future periods are presented in Figures 8 and 9. Bio-18 ranges from 270 to 1000 mm, and Bio-19 ranges from 0 to 900 mm for the historical period. The highest Bio-18 was in northern Myanmar and southeastern SEA, ranging from 800 to 1100 mm. The lowest Bio-19 was in Myanmar and Thailand, ranging from 0 to 300 mm.

For Bio-18, the projected MME mean showed the same distribution for the two scenarios, with a decrease in Bio-18 in most of SEA by 15.5%, except for northern Indonesia and Myanmar, Brunei, and the southeastern islands, where it increased by 17.4%. For Bio-19,

the MME mean showed an average increase of 19%, while a decrease of 32% in northern Myanmar and the southern coastal region. The highest increase was observed in southern Myanmar for the far future of SSP5-8.5. The 5th and 95th percentile for Bio-18 illustrated the highest uncertainty in the mainland of SEA. It showed the largest decrease of −95% for the 5th percentile and the largest increase of 205% for the 95th percentile. For Bio-19, the 5th percentile maps showed the lowest decrease in Malaysia, Indonesia, Brunei, and the southwestern islands by 99.5%. The 95th percentile showed the highest increase in southern Myanmar by 700% for both far futures of the two scenarios.

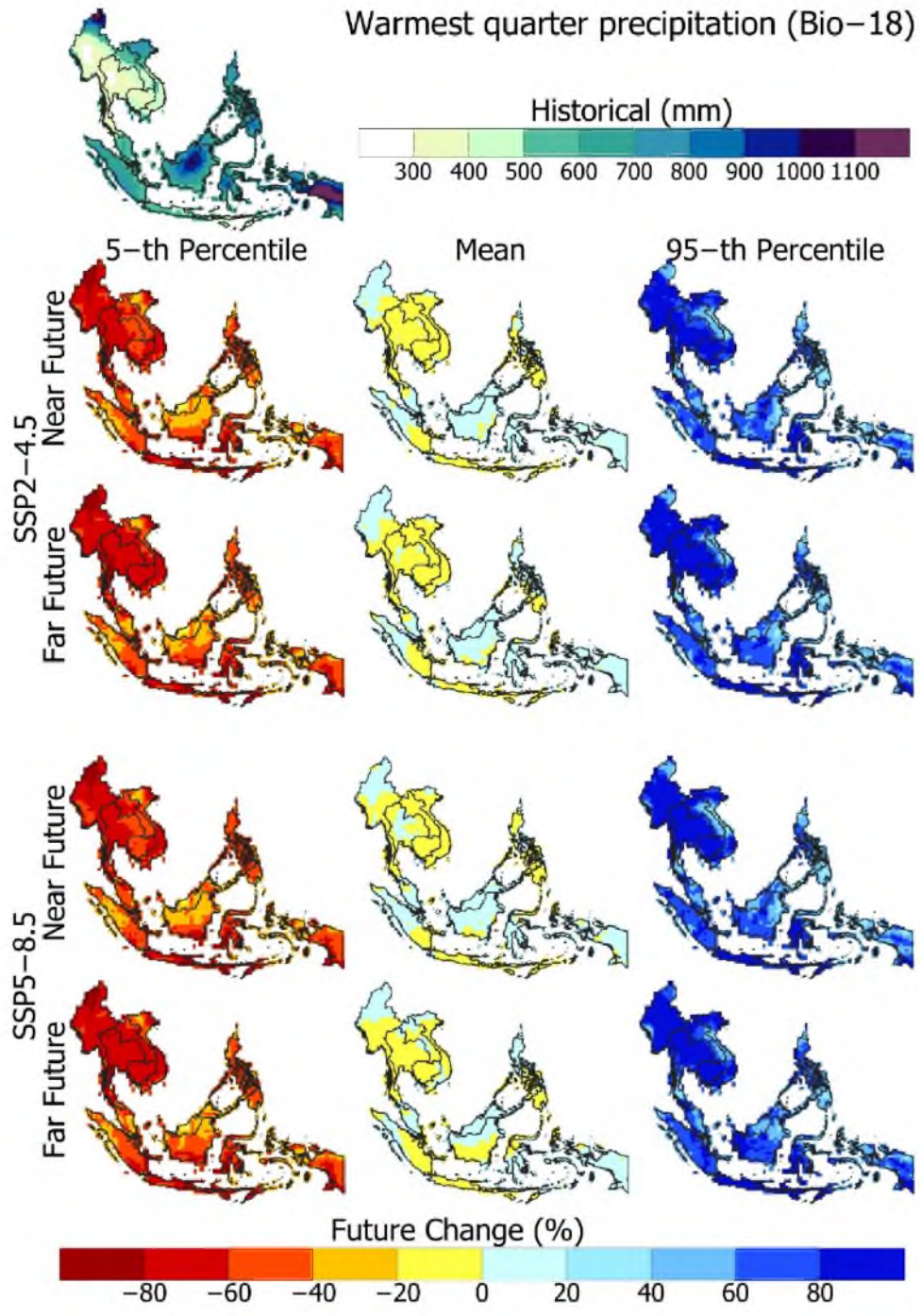

Figure 8. Spatial distribution of historical mean precipitation of warmest quarter (Bio-18) and its changes in the near and far futures for SSP2-4.5 and SSP5-8.5.

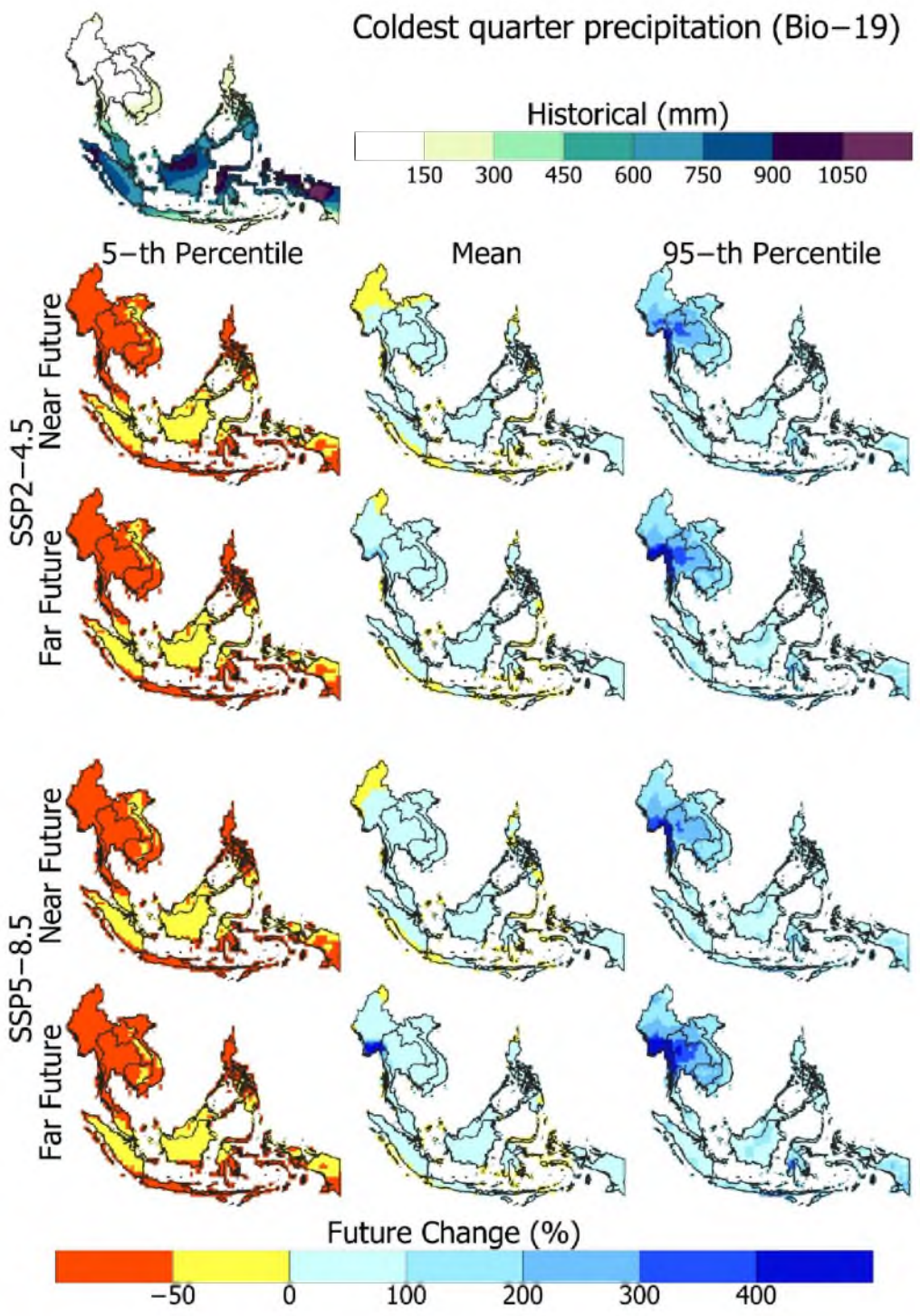

Figure 9. Spatial distribution of historical mean precipitation of coldest quarter (Bio-19) and its changes in the near and far futures for SSP2-4.5 and SSP5-8.5.

The summary of the changes in the precipitation-bioclimatic indicators over SEA is presented in Table 3. The results revealed an increase in most indicators over most SEA, except Bio-14, Bio-17, and Bio-18. The Bio-14 was projected to decrease over most SEA, whereas the Bio-17 and Bio-18 showed both an increase and decrease, respectively. In addition, several indicators showed a decrease in the southern coastal region.

Table 3. Summary of the changes in the precipitation-bioclimatic indicators in this study.

Indicator	Changes	
	Increase	**Decrease**
	Annual indicators	
Bio-12 Annual precipitation	All over SEA, except the southern and eastern coastal regions	Southern and eastern coastal region
	Monthly indicator	
Bio-13 Precipitation in the wettest month	All over SEA, except the middle southern coastal region, the highest increase in Myanmar	Central southern coastal region
Bio-14 Precipitation in the driest month	South Myanmar, Thailand, Cambodia, Brunei, and northwestern Indonesia	All over SEA, except southern Myanmar, Thailand, Cambodia, Brunei, and northwestern Indonesia
	Seasonal indicator	
Bio-15 Precipitation seasonality	All over SEA, mostly at the same rate	-
Bio-16 Precipitation in the wettest quarter	All over SEA, mostly at the same rate	Southern and eastern coastal region
Bio-17 Precipitation in the driest quarter	Thailand, Indonesia, and the southeastern island	Southern and western coastal region and the Philippines
Bio-18 Precipitation in the warmest quarter	North Myanmar, Brunei, and the southeastern islands	Southern coastal region and the mainland of SEA, except for northern Myanmar.
Bio-19 Precipitation in the coldest quarter	All over SEA, the higher increase in southern Myanmar	Northern Myanmar, southern and eastern coastal region

5. Discussion

Examining a region's climate is one of the best ways to gauge its bio-environment. As a result, bioclimate patterns can be utilized to foretell how a region's biodiversity would likely shift in the future. Changes in different climate variables have been widely evaluated in SEA as a whole and in different countries of the region individually; however, those variables were inadequate to decipher the specific factors determining biological and ecological changes. This study evaluated the changes in precipitation indicators of WorlcClim, which can explain the climatic influence on a species' physiology; therefore, projections of the indicators can help evaluate climate change impacts on the bio-environment in SEA in the future.

The present study showed an increase in annual rainfall by 6–12.4% in most SEA, which agree with [39] which projected the rainfall under the same predecessor version of scenarios SSP2-4.5 and SSP5-8.5. The increases were also projected for the wettest and driest months. Large-scale atmospheric phenomena such as the mid-Julian oscillation (MJO) and cold surge (CS) and their interactions with in situ-synoptic systems have an impact on the climate of the SEA [40,41]. The highest rainfall occurs in years when both a CS and MJO occur [42]. Global temperature caused stronger and more frequent MJO [12]. The warming effect in Siberia has also increased the recurrence of CSs in SEA [42]. The higher recurrence of CSs and MJOs may cause an increase in rainfall in the region; however, the present study revealed that the impact of increasing frequency of CSs and MJOs is still not visible in the study area.

This study also projected a 5.5 and 6.4% decrease in rainfall in southern SEA and the Philippines for SSP2-4.5. Sa'adi et al. [43] evaluated the changes in rainfall in southern SEA and found no change in rainfall, though there was a reported rise in rainfall over all of SEA. They argued that this might be due to the effect of increasing CSs and MJOs in the region; however, they used GCMs of CMIP5. Similar disagreement was found with the results of Ngai, et al. [44]. They showed an increased rainfall over all of SEA. This may also be due to the use of CMIP5 models in precipitation projections. Hamed, et al. [45] showed the discrepancy in rainfall projections using CMIP5 and CMIP6 GCMs in SEA. Their study showed a rainfall decrease for both SSPs; however, the decrease would be smaller for SSP2-4.5 than for SSP5-8.5. This agrees with Pradana and Utaminingsih [46]. They also reported wetter conditions for a moderate scenario than for a worst-case scenario.

A major finding of this study is the increase in precipitation seasonality over SEA by 0.0 to 6.0% in the near future which can be increased up to 8% in the far future. This is due to an increase in rainfall in the wettest quarter by 2.85% while a decrease in the driest quarter by 1.0%. This agrees with Tangang, et al. [39]. They showed a decrease in rainfall during December–February (wettest quarter) while an increase during June–August (driest quarter). They also showed a major precipitation reduction over the maritime continent, as found in the present study. The seasonal variability of rainfall in most of SEA is less. The present study revealed that climate change would make the rainfall in SEA more seasonal in the future. The results agree with Kang, et al. [47]. They showed increased precipitation seasonality over maritime SEA. Supari, et al. [48] also suggested stronger precipitation seasonality over SEA in the future. This study's overall finding also agrees with a previous study [49] based on the multimodel simulations of the Southeast Asia regional climate projections under a global warming of 2 °C. The article gives thorough information on the expected changes in annual precipitation extremes over Southeast Asia. The results showed apprehension in northern Myanmar that the region could be hit harder than other parts of Southeast Asia.

6. Conclusions

This study projected possible future changes in eight precipitation bioclimatic indicators over SEA with related uncertainties. 23 GCMs projections were used for the 90% CI and mean MME. The study found an increase in the mean annual and seasonal precipitation over SEA. The main increase in the precipitation would be in the coldest and wettest quarters for both scenarios, especially in Myanmar and Thailand. On the other hand, some parts, such as Indonesia, would experience a decrease in precipitation. Ecological, agricultural, and water resource management can benefit from the maps depicting the geographical patterns of precipitation bioclimatic indicators and their future projections developed in this work. In addition, the governments of SEA might use it as part of their sustainable development plans. Only medium and high (SSP2-4.5 and 5-8.5) pathways were considered in this study for the future projection of bioclimatic indicators. SSP1-1.9, 1-2.6, and 3-7.0 may be utilized in the future. As a future work, it is also recommended to forecast how climate change would affect the potential migration of different species over time. As a result of these changes, models can be created to analyze the influence on Southeast Asia's bio-environment.

Supplementary Materials: The following supporting information can be downloaded at: https://www.mdpi.com/article/10.3390/su142013596/s1, Figure S1: Spatial distribution of historical annual precipitation (Bio-12) and changes in the near and far futures for SSP2-4.5 and SSP5-8.5 using ACCESS-CM2; Figure S2: Spatial distribution of historical precipitation of the wettest month (Bio-13) and changes in the near and far futures for SSP2-4.5 and SSP5-8.5 using ACCESS-CM2; Figure S3: Spatial distribution of historical precipitation of the driest month (Bio-14) and changes in the near and far futures for SSP2-4.5 and SSP5-8.5 using ACCESS-CM2; Figure S4: Spatial distribution of historical precipitation seasonality (Bio-15) and changes in the near and far futures for SSP2-4.5 and SSP5-8.5 using ACCESS-CM2; Figure S5: Spatial distribution of historical precipitation of the wettest quarter (Bio-16) and changes in the near and far futures for SSP2-4.5 and SSP5-8.5 using ACCESS-CM2; Figure S6: Spatial distribution of historical precipitation of the driest quarter (Bio-17) and changes in the near and far futures for SSP2-4.5 and SSP5-8.5 using ACCESS-CM2; Figure S7: Spatial distribution of historical precipitation of the warmest quarter (Bio-18) and changes in the near and far futures for SSP2-4.5 and SSP5-8.5 using ACCESS-CM2; Figure S8: Spatial distribution of historical precipitation of the coldest quarter (Bio-19) and changes in the near and far futures for SSP2-4.5 and SSP5-8.5 using ACCESS-CM2.

Author Contributions: Conceptualization, M.T.S., M.M.H. and M.S.N.; methodology, M.T.S. and M.M.H.; software, M.T.S. and M.M.H.; validation, M.T.S., M.M.H., and S.S.; formal analysis, M.M.H.; investigation, M.M.H. and M.S.N.; resources, M.T.S. and M.M.H.; data curation, M.T.S. and M.M.H.; writing—original draft preparation, M.T.S., M.M.H., M.S.N. and S.S.; writing—review and editing, M.S.N. and S.S.; visualization, M.M.H.; supervision, M.S.N. and S.S.; project administration, M.S.N.

and S.S.; funding acquisition, M.S.N. All authors have read and agreed to the published version of the manuscript.

Funding: Authors are grateful to Universiti Teknologi Malaysia (UTM) for providing financial support to conduct this research through the UTM High Impact Research Grant No. 09G07.

Institutional Review Board Statement: Not applicable.

Informed Consent Statement: Not applicable.

Data Availability Statement: Not applicable.

Conflicts of Interest: The authors declare no conflict of interest.

References

1. O'Donnell, M.S.; Ignizio, D.A. Bioclimatic predictors for supporting ecological applications in the conterminous United States. *US Geol. Surv. Data Ser.* **2012**, *691*, 4–9.
2. Huang, X.-H.; Zhou, Y.-Z.; Fang, J.-P.; Hou, L. Climate change has more adverse impacts on the higher mountain communities than the lower ones: People's perception from the northern Himalayas. *J. Mt. Sci.* **2019**, *16*, 2625–2639. [CrossRef]
3. Ebrahimi, A.; Abbasi, A.O.; Liang, J.; Jacobs, D.F. Spatiotemporal trends of black walnut forest stocking under climate change. *Front. For. Glob. Chang.* **2022**, *10*. [CrossRef]
4. Zhao, H.; Jia, G.; Xu, X.; Zhang, A. Contrasting Responses of Vegetation Production to Rainfall Anomalies Across the Northeast China Transect. *J. Geophys. Res. Biogeosciences* **2022**, *127*, e2022JG006842. [CrossRef]
5. Charalampopoulos, I.; Tsiros, I. A preliminary study on the effect of rainfall events on human thermal comfort under hot weather conditions. In *Perspectives on Atmospheric Sciences*; Springer: Berlin/Heidelberg, Germany, 2017; pp. 329–334.
6. Flohr, B.; Ouzman, J.; McBeath, T.; Rebetzke, G.; Kirkegaard, J.; Llewellyn, R. Redefining the link between rainfall and crop establishment in dryland cropping systems. *Agric. Syst.* **2021**, *190*, 103105. [CrossRef]
7. Liu, J.; Burgess, K.S.; Ge, X. Species pool size and rainfall account for the relationship between biodiversity and biomass production in natural forests of China. *Ecol. Evol.* **2022**, *12*, e8838. [CrossRef]
8. Simba, L.D.; Pryke, J.S.; Roets, F.; Seymour, C.L. Interactive effects of rangeland management and rainfall on dung beetle diversity. *Biodivers. Conserv.* **2022**, *31*, 2639–2656. [CrossRef]
9. Shahid, S. Probable Impacts of Climate Change on Public Health in Bangladesh. *Asia Pac. J. Public Health* **2010**, *22*, 310–319. [CrossRef]
10. Peirce, A.M.; Espira, L.M.; Larson, P.S. Climate Change Related Catastrophic Rainfall Events and Non-Communicable Respiratory Disease: A Systematic Review of the Literature. *Climate* **2022**, *10*, 101. [CrossRef]
11. Jassim, M.S.; Coskuner, G.; Munir, S. Temporal analysis of air pollution and its relationship with meteorological parameters in Bahrain, 2006–2012. *Arab. J. Geosci.* **2018**, *11*, 62. [CrossRef]
12. IPCC. *Climate Change 2014: Impacts, Adaptation, and Vulnerability*; Cambridge University Press: Cambridge, UK; New York, NY, USA, 2014; p. 1132.
13. Hamed, M.M.; Nashwan, M.S.; Shahid, S.; Ismail, T.B.; Dewan, A.; Asaduzzaman, M. Thermal bioclimatic indicators over Southeast Asia: Present status and future projection using CMIP6. *Environ. Sci. Pollut. Res. Int.* **2022**, 1–20. [CrossRef] [PubMed]
14. Strang, K.; Rusli, N. The Challenges of Conserving Biodiversity: A Spotlight on Southeast Asia. In *Wildlife Biodiversity Conservation*; Springer: Berlin/Heidelberg, Germany, 2021; pp. 47–66.
15. Nuttall, M.N.; Griffin, O.; Fewster, R.M.; McGowan, P.J.K.; Abernethy, K.; O'Kelly, H.; Nut, M.; Sot, V.; Bunnefeld, N. Long-term monitoring of wildlife populations for protected area management in Southeast Asia. *Conserv. Sci. Pract.* **2021**, *4*, e614. [CrossRef]
16. Dadap, N.C.; Cobb, A.R.; Hoyt, A.M.; Harvey, C.F.; Feldman, A.F.; Im, E.-S.; Konings, A.G. Climate change-induced peatland drying in Southeast Asia. *Environ. Res. Lett.* **2022**, *17*, 074026. [CrossRef]
17. Supharatid, S.; Nafung, J.; Aribarg, T. Projected changes in temperature and precipitation over mainland Southeast Asia by CMIP6 models. *J. Water Clim. Chang.* **2022**, *13*, 337–356. [CrossRef]
18. Yong, D.L.; Kee, J.Y.; Aung, P.P.; Jain, A.; Yeap, C.-A.; Au, N.J.; Jearwattanakanok, A.; Lim, K.K.; Yu, Y.-T.; Fu, V.W.K. Conserving migratory waterbirds and the coastal zone: The future of South-east Asia's intertidal wetlands. *Oryx* **2022**, *56*, 176–183. [CrossRef]
19. Zhongming, Z.; Linong, L.; Xiaona, Y.; Wangqiang, Z.; Wei, L. Climate Change a Bigger Threat to Landscape Biodiversity than Emerald Ash Borer. Global S&T Development Trend Analysis Platform of Resources and Environment. 2021. Available online: http://119.78.100.173/C666/handle/2XK7JSWQ/329064 (accessed on 29 September 2022).
20. Saijuntha, W.; Petney, T.N. The Changing Biodiversity of Parasite Hosts in Southeast Asia. In *Biodiversity of Southeast Asian Parasites and Vectors Causing Human Disease*; Springer: Berlin/Heidelberg, Germany, 2021; pp. 1–15.
21. Kamworapan, S.; Surussavadee, C. Evaluation of CMIP5 Global Climate Models for Simulating Climatological Temperature and Precipitation for Southeast Asia. *Adv. Meteorol.* **2019**, *2019*, 1067365. [CrossRef]
22. Eckstein, D.; Künzel, V.; Schäfer, L. *Global Climate Risk Index 2018*; Germanwatch: Berlin/Heidelberg, Germany, 2017.
23. Alvarado-Serrano, D.F.; Knowles, L.L. Ecological niche models in phylogeographic studies: Applications, advances and precautions. *Mol. Ecol. Resour.* **2013**, *14*, 233–248. [CrossRef]

24. Hijmans, R.J.; Cameron, S.E.; Parra, J.L.; Jones, P.G.; Jarvis, A. Very high resolution interpolated climate surfaces for global land areas. *Int. J. Climatol. J. R. Meteorol. Soc.* **2005**, *25*, 1965–1978. [CrossRef]
25. Title, P.O.; Bemmels, J.B. ENVIREM: An expanded set of bioclimatic and topographic variables increases flexibility and improves performance of ecological niche modeling. *Ecography* **2018**, *41*, 291–307. [CrossRef]
26. Booth, T.H. Checking bioclimatic variables that combine temperature and precipitation data before their use in species distribution models. *Austral Ecol.* **2022**, *47*, 1506–1514. [CrossRef]
27. Otgonbayar, M.; Atzberger, C.; Sumiya, E.; Dalantai, S.; Chambers, J. Estimation of bioclimatic variables of Mongolia derived from remote sensing data. *Front. Earth Sci.* **2022**, *16*, 323–339. [CrossRef]
28. Cerasoli, F.; D'Alessandro, P.; Biondi, M. Worldclim 2.1 versus Worldclim 1.4: Climatic niche and grid resolution affect between-version mismatches in Habitat Suitability Models predictions across Europe. *Ecol. Evol.* **2022**, *12*, e8430. [CrossRef] [PubMed]
29. Almazroui, M.; Islam, M.N.; Saeed, S.; Saeed, F.; Ismail, M. Future Changes in Climate over the Arabian Peninsula based on CMIP6 Multimodel Simulations. *Earth Syst. Environ.* **2020**, *4*, 611–630. [CrossRef]
30. O'Neill, B.C.; Tebaldi, C.; van Vuuren, D.P.; Eyring, V.; Friedlingstein, P.; Hurtt, G.; Knutti, R.; Kriegler, E.; Lamarque, J.-F.; Lowe, J.; et al. The Scenario Model Intercomparison Project (ScenarioMIP) for CMIP6. *Geosci. Model Dev.* **2016**, *9*, 3461–3482. [CrossRef]
31. Eyring, V.; Bony, S.; Meehl, G.A.; Senior, C.A.; Stevens, B.; Stouffer, R.J.; Taylor, K.E. Overview of the Coupled Model Intercomparison Project Phase 6 (CMIP6) experimental design and organization. *Geosci. Model Dev.* **2016**, *9*, 1937–1958. [CrossRef]
32. Moss, R.H.; Edmonds, J.A.; Hibbard, K.A.; Manning, M.R.; Rose, S.K.; van Vuuren, D.P.; Carter, T.R.; Emori, S.; Kainuma, M.; Kram, T.; et al. The next generation of scenarios for climate change research and assessment. *Nature* **2010**, *463*, 747–756. [CrossRef]
33. Zhu, X.; Lee, S.-Y.; Wen, X.; Ji, Z.; Lin, L.; Wei, Z.; Zheng, Z.; Xu, D.; Dong, W. Extreme climate changes over three major river basins in China as seen in CMIP5 and CMIP6. *Clim. Dyn.* **2021**, *57*, 1187–1205. [CrossRef]
34. Iqbal, Z.; Shahid, S.; Ahmed, K.; Ismail, T.; Ziarh, G.F.; Chung, E.-S.; Wang, X. Evaluation of CMIP6 GCM rainfall in mainland Southeast Asia. *Atmospheric Res.* **2021**, *254*, 105525. [CrossRef]
35. Hamed, M.M.; Nashwan, M.S.; Shahid, S. A novel selection method of CMIP6 GCMs for robust climate projection. *Int. J. Clim.* **2022**, *42*, 4258–4272. [CrossRef]
36. Li-Juan, M.; Miao, L.-J.; Jiang, Z.-H.; Wang, G.-J.; Gnyawali, K.R.; Zhang, J.; Zhang, H.; Fang, K.; He, Y.; Li, C. Projected drought conditions in Northwest China with CMIP6 models under combined SSPs and RCPs for 2015–2099. *Adv. Clim. Chang. Res.* **2020**, *11*, 210–217.
37. Salehie, O.; bin Ismail, T.; Hamed, M.M.; Shahid, S.; Muhammad, M.K.I. Projection of Hot and Cold Extremes in the Amu River Basin of Central Asia using GCMs CMIP6. *Stoch. Hydrol. Hydraul.* **2022**, 1–22. [CrossRef]
38. Bede-Fazekas, Á.; Somodi, I. The way bioclimatic variables are calculated has impact on potential distribution models. *Methods Ecol. Evol.* **2020**, *11*, 1559–1570. [CrossRef]
39. Tangang, F.; Chung, J.X.; Juneng, L.; Supari; Salimun, E.; Ngai, S.T.; Jamaluddin, A.F.; Mohd, M.S.F.; Cruz, F.; Narisma, G.; et al. Projected future changes in rainfall in Southeast Asia based on CORDEX–SEA multi-model simulations. *Clim. Dyn.* **2020**, *55*, 1247–1267. [CrossRef]
40. Hoell, A.; Cannon, F.; Barlow, M. Middle East and Southwest Asia Daily Precipitation Characteristics Associated with the Madden–Julian Oscillation during Boreal Winter. *J. Clim.* **2018**, *31*, 8843–8860. [CrossRef]
41. Xavier, P.; Rahmat, R.; Cheong, W.K.; Wallace, E. Influence of Madden-Julian Oscillation on Southeast Asia rainfall extremes: Observations and predictability. *Geophys. Res. Lett.* **2014**, *41*, 4406–4412. [CrossRef]
42. Lim, S.Y.; Marzin, C.; Xavier, P.; Chang, C.-P.; Timbal, B. Impacts of Boreal Winter Monsoon Cold Surges and the Interaction with MJO on Southeast Asia Rainfall. *J. Clim.* **2017**, *30*, 4267–4281. [CrossRef]
43. Sa'adi, Z.; Shahid, S.; Ismail, T.; Chung, E.-S.; Wang, X.-J. Trends analysis of rainfall and rainfall extremes in Sarawak, Malaysia using modified Mann–Kendall test. *Meteorol. Atmos. Phys.* **2019**, *131*, 263–277. [CrossRef]
44. Ngai, S.T.; Juneng, L.; Tangang, F.; Chung, J.X.; Supari, S.; Salimun, E.; Cruz, F.; Ngo-Duc, T.; Phan-Van, T.; Santisirisomboon, J.; et al. Projected mean and extreme precipitation based on bias-corrected simulation outputs of CORDEX Southeast Asia. *Weather. Clim. Extrem.* **2022**, *37*, 100484. [CrossRef]
45. Hamed, M.M.; Nashwan, M.S.; Shahid, S.; Ismail, T.b.; Wang, X.-j.; Dewan, A.; Asaduzzaman, M. Inconsistency in historical simulations and future projections of temperature and rainfall: A comparison of CMIP5 and CMIP6 models over Southeast Asia. *Atmos. Res.* **2022**, *265*, 105927. [CrossRef]
46. Pradana, R.P.; Utaminingsih, W. *Future Precipitation Projections and Its Potential Impact for Development and Management of Irrigation over Indonesia*; 3rd World Irrigatin Forum (WIF3): Bali, Indonesia, 2019.
47. Kang, S.; Im, E.-S.; Eltahir, E.A.B. Future climate change enhances rainfall seasonality in a regional model of western Maritime Continent. *Clim. Dyn.* **2019**, *52*, 747–764. [CrossRef]
48. Supari; Tangang, F.; Juneng, L.; Cruz, F.; Chung, J.X.; Ngai, S.T.; Salimun, E.; Mohd, M.S.F.; Santisirisomboon, J.; Singhruck, P.; et al. Multi-model projections of precipitation extremes in Southeast Asia based on CORDEX-Southeast Asia simulations. *Environ. Res.* **2020**, *184*, 109350. [CrossRef] [PubMed]
49. Tangang, F.; Supari, S.; Chung, J.X.; Cruz, F.; Salimun, E.; Ngai, S.T.; Juneng, L.; Santisirisomboon, J.; Santisirisomboon, J.; Ngo-Duc, T. Future changes in annual precipitation extremes over Southeast Asia under global warming of 2 C. *APN Sci. Bull.* **2018**, 8. [CrossRef]